Available online at www.sciencedirect.com
SCIENCE DIRECT®
Applied Catalysis A: General 253 (2003) 257–269
APPLIED CATALYSIS A: GENERAL
www.elsevier.com/locate/apcata

Synthesis and characterization of ZSM-5 coatings onto cordierite honeycomb supports

M.A. Ulla [a], R. Mallada [b], J. Coronas [b], L. Gutierrez [a], E. Miró [a], J. Santamaría [b,*]

[a] *INCAPE (FIQ, UNL-CONICET), Santiago del Estero 2829, 3000 Santa Fe, Argentina*
[b] *Department of Chemical Engineering, Faculty of Science, University of Zaragoza, 50009 Zaragoza, Spain*

Received 2 May 2003; received in revised form 18 June 2003; accepted 19 June 2003

Abstract

Zeolite ZSM-5 layers (up to ca. 30% by weight) have been synthesized on cordierite substrates, following either a direct hydrothermal synthesis procedure or a secondary growth method, in this case after seeding of the support. The Si/Al ratio in the synthesis gel ranged from 14 to 100, but layers with a high Al content (i.e. a low Si/Al ratio) could not be prepared directly on the cordierite support. However, MFI layers with a low Si/Al ratio were readily grown after depositing an intermediate Si-rich layer. The results also show that the Si/Al ratio of the synthesis gel has a direct effect on the morphology, crystallinity and orientation of the MFI layer formed.
© 2003 Elsevier B.V. All rights reserved.

Keywords: Zeolite coatings; Monolith substrates; Si/Al ratio

1. Introduction

A low pressure drop, and often also a good tolerance to plugging by dust, are essential requisites for end-of-pipe catalytic applications [1–3]. This has led to the use of ceramic and metal-based catalytic monoliths for a wide variety of gas phase reactions such as three-way catalysis and diesel catalysis in automotive applications, ozone abatement in aircrafts and automobiles, selective reduction of NO_x and catalytic combustion for organic pollutants and odor removal. With ceramic monoliths, the support structure is made of a non-catalytic, thermally resistant material, typically cordierite, onto which a catalytic layer (e.g. γ-alumina) is deposited. The usual coating techniques are dip-coating, slip-coating and spin-coating [4]. However, as noted by Heck et al. [2], the amount of catalyst that can be deposited in this way for a given reactor volume is much less than for a comparable volume in a fixed bed. Thus, for many reacting systems, the monolith may not contain sufficient catalyst to give the desired yields.

Among the alternatives being considered to solve this problem is the use of catalytically active materials to manufacture the monolith, although this presents considerable problems regarding the mechanical stability of the final product. Another possibility concerns the deposition of active materials directly on the support, (i.e. without a previous washcoat). Zeolites are the main candidates for this approach due to the considerable experience accumulated in recent years concerning the synthesis of zeolite films on different substrates. This knowledge has been applied to the development of sensors, optoelectronic devices and

* Corresponding author. Tel.: +34-976-761153; fax: +34-976-762142.
E-mail address: iqcatal@unizar.es (J. Santamaría).

0926-860X/$ – see front matter © 2003 Elsevier B.V. All rights reserved.
doi:10.1016/S0926-860X(03)00498-8

membranes (see for instance the reviews [4,5]) and also as coatings for monolith structures, ceramic foams and metal gauzes [1,6–12]. These have normally been aimed towards catalytic applications, although in a recent work [13] a zeolite membrane was prepared on a monolith structure and used for the gas phase separation of hydrocarbon isomers. A variety of synthesis methods has been applied to obtain zeolite films on ceramic supports, from a simple washcoating of zeolite particles followed by a stabilizing thermal treatment, to complex hydrothermal synthesis. One of the benefits of the different hydrothermal synthesis methods (direct synthesis, seeded growth, vapor-phase synthesis) compared to washcoating of zeolite particles is a stronger adhesion of the coating to the support, a feature required to withstand vibrations in mobile applications.

The main reason for using zeolites films is obviously the high activity and selectivity of zeolites for many interesting reactions. In particular, transition-metal ion-exchanged zeolites (Si/Al ratio: 100–7) have performed efficiently in gas phase reaction systems such as NO_x reduction, VOC combustion and selective oxidations [14–17]. In addition, zeolite coatings have the advantage of being synthesized directly on the channel surface, which avoids the use of a washcoat, and also of binders [3,10], giving a higher active load per gram of coating. The direct synthesis of zeolite coatings therefore appears as an interesting alternative to provide a sufficient active load on monolith substrates.

In spite of this, only few investigations dealing with this type of synthesis can be found in the literature. In particular, the relationship between the Si/Al ratio in the synthesis gel and the characteristics of the resulting zeolite coating on the monolith have been scarcely investigated. It is known, however, that the first step in hydrothermal synthesis of zeolite films is the formation of a precursor gel layer onto the substrate, which serves as the primary source of nuclei [18]. The addition of aluminum to the solution accelerates gel layer formation but retards the nucleation and zeolitization processes within it [18,19]. From the point of view of catalyst preparation a high ion exchange capability is desirable, and thus synthesis gels with a high Al content are preferred. However, as mentioned above, the use of Al-rich synthesis gels has a direct influence on the kinetics of the process and as a consequence, high loadings (on a weight or volume basis) of well-crystallized zeolite films are difficult to obtain. Another important factor regarding the use of zeolite coatings in catalytic applications is the accessibility of the active sites within the zeolite framework. MFI zeolite crystals have straight, nearly circular (0.53 nm × 0.56 nm) channels running along the *b*-direction, and zig-zag elliptic (0.51 nm × 0.55 nm) channels along the *a*-axis, while there are no channels along the *c*-direction. Therefore, zeolite films consisting of intergrown crystals with either *a*- or *b*-axes perpendicular to the support, or films with a random orientation of the constituent crystals would have a greater accessibility, compared to *c*-oriented films. Preferential orientation is often found during the preparation of zeolite films and membranes, and the orientation of the crystals seems to depend on the characteristics of the support, but also on the conditions of crystal growth (seeding, temperature, gel composition).

The aim of this work is to gain further insight on the relationship between the aluminum content in the precursor solution and the properties of ZSM-5 films on ceramic (cordierite) monoliths. To this end, precursor solutions with different Si/Al ratios (100, 35 and 14) were used for hydrothermal synthesis (both direct synthesis and seeded growth methods). The films obtained have been compared regarding zeolite loading, morphology, crystallinity and preferred orientation of crystals.

2. Experimental

2.1. Synthesis

Cordierite ($2MgO–2Al_2O_3–5SiO_2$) honeycomb monoliths (Corning, 400 cells/in.^{2}, 0.1 mm average wall thickness) were used as substrates. The monolith density and its external specific area were 1554 kg m^{-3} and 3650 m^2 m^{-3}, respectively. The growth of ZSM-5 films onto these substrates was carried out by either (i) direct hydrothermal synthesis (also termed in situ growth), or (ii) hydrothermal synthesis after seeding the surface of the substrate (also termed *secondary growth*). For seeding, a colloidal suspension of silicalite seeds (20 g/l) was prepared, with an average crystal size of 120 nm. The seeds were obtained by hydrothermal synthesis at 125 °C

Table 1
Hydrothermal synthesis of ZSM-5 with different Si/Al ratio

Precursor solution composition					Synthesis conditions		
Si/Al	H_2O/Si	Na/Si	Template/Si	Template	Temperature (°C)	Time (h)	Reference
100	47	0.143	0.048	TPAOH	150	8	[20]
35	46	0.130	0.043	TPABr	185	24	[21]
14	46	0.130	0.043	TPABr	180	24	This work

for 8 h using a synthesis solution with a molar composition of $25SiO_2$:$333H_2O$:2.125NaOH:6TPAOH, where TPAOH refers to tetrapropylammonium hydroxide. Seeding was accomplished by dipping the cordierite substrates in the colloidal suspension of seed particles, then drying in air at room temperature for 3 h. The dipping and drying steps were repeated three times. The weight gain of the seeded substrates was around 3–4%.

Three ZSM-5 precursor solutions with different Si/Al ratio (100, 35 and 14, respectively) were used for hydrothermal synthesis. Their molar compositions and the synthesis conditions used reported in Table 1. Before synthesis, the substrates were wrapped with Teflon tape on the outside, fixed to a Teflon holder and placed vertically with their channels aligned parallel to the main axis of the autoclave. The autoclave was then filled with the corresponding precursor solution (30 ml) and placed in a convection oven at the desired temperature. After synthesis, the substrates were rinsed with distilled water, washed in ultrasonic bath for 20 min to remove any loosely adhering material, and then dried in a furnace at 120 °C. Table 2 summarizes the main characteristics of the film coated substrates, the method of ZSM-5 growth, the Si/Al ratio in the synthesis gel, the weight gain and the specific surface area after synthesis.

In the case of in situ growth (unseeded substrates), the synthesis cycle was repeated twice, giving the final percentage weight gains of Table 2. The composition of the solutions used were the same as for secondary growth, given in Table 1.

In the remainder of this work, substrates coated by the direct synthesis are denoted by Dnn, where nn is the Si/Al ratio in the synthesis gel. In the same way, the substrates prepared by secondary synthesis

Table 2
Characteristics of the samples prepared

Film coated substrate	Synthesis method	Si/Al ratio	Number synthesis cycles	Weight gain (%)	S_t (m^2/g)[a]	S_z (m^2/g)[b]
D100	Direct	100	2	8.3	22.7	278.3
S100	Secondary	100	1	18.0	58.2	321.0
D35	Direct	35	2	14.8	41.7	278.7
S35	Secondary	35	1	15.1	46.1	321.5
S35V[c]	Secondary	35	1	19.0	59.9	297.6
S14	Secondary	14	1	15.5	–	–
S14V[c]	Secondary	14	1	14.2	–	–
S100,14[d]	Secondary	100	1	16.8	80.8	268.3
		14	1	12.1	80.8	268.3
Cordierite support	–	–	–	–	0.5	–

[a] Specific surface, referred to the total (monolith + zeolite layer) weight.
[b] Specific surface, referred to the zeolite weight.
[c] After the hydrothermal synthesis, the film coated substrates were treated with steam under autogenous pressure in an autoclave at 180 °C for 24 h.
[d] A gel precursor with Si/Al = 100 was used for the first hydrothermal synthesis on a seeded substrate and then a second synthesis was carried out with Si/Al = 14.

are denoted by Snn. Some of the samples prepared by secondary synthesis were subjected to a 24 h treatment under steam in an autoclave at 180 °C. These are denoted as SnnV. Finally, for the sample named S100,14 a mixed synthesis was used: first, a secondary synthesis was carried out using a gel with a Si/Al ratio equal to 100, then the sample was subjected to a second synthesis using a gel with a Si/Al ratio equal to 14.

2.2. Characterization

The surface and cross-sections of ZSM-5 coated substrates were examined by Scanning Electron Microscopy (JEOL JSM 6400) operated at 20 kV. The Si/Al ratio profiles were measured using an energy-dispersive X-ray analysis (EDX) system attached to the SEM instrument. X-ray diffraction patterns of the films and of the residual powder collected at the bottom of autoclaves after synthesis were obtained with a diffractometer using a Cu Kα radiations (Rygaku/Max System). Finally, the surface area of the coated substrates was estimated by BET analysis (Micromeritics, Pulse Chemisorb 2700) using N_2 adsorption. Blank experiments with the cordierite support allowed a separate estimation of its contribution.

3. Results and discussion

3.1. Zeolite powder

The residual zeolite powder obtained after all hydrothermal syntheses presented a clear ZSM-5 structure. Fig. 1 shows the XRD patterns for the three different Si/Al ratios. Some contribution of amorphous phase is detected for Si/Al = 14, in agreement with the already mentioned retardation of nucleation and crystallization processes in the presence of higher Al contents [18,19].

3.2. ZSM-5 coated substrates: Si/Al = 100

The XRD patterns of the film-coated substrates after in situ growth (D100) and secondary growth (S100) are shown in Fig. 2, where the signals associated to the cordierite substrate are identified with a star. Both diffractograms show the presence of the most characteristic ZSM-5 peaks and the absence of significant amounts of other zeolite phases, indicating that essentially pure ZSM-5 had formed on the cordierite support.

Fig. 3 shows micrographs with different views of the D100 sample. Well-developed crystals with the

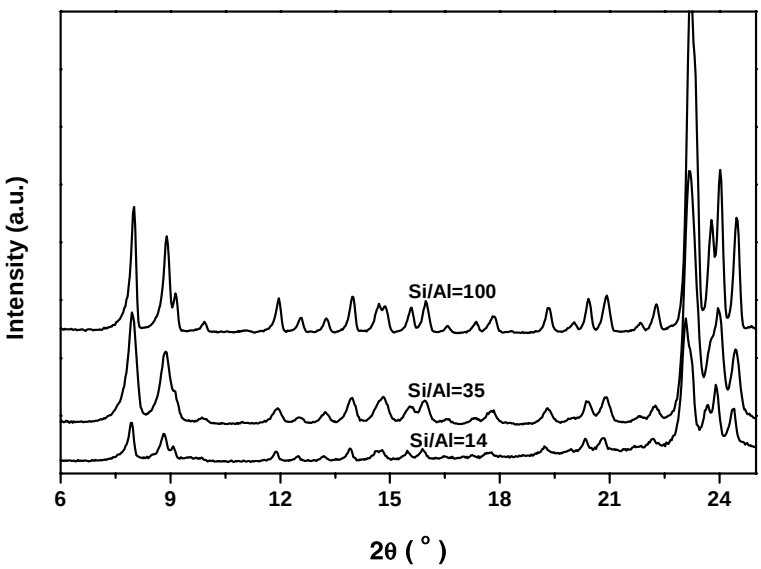

Fig. 1. X-ray diffraction patterns of ZSM-5 powders with Si/Al: 100, 35 and 14. Hydrothermal synthesis conditions are given in Table 1.

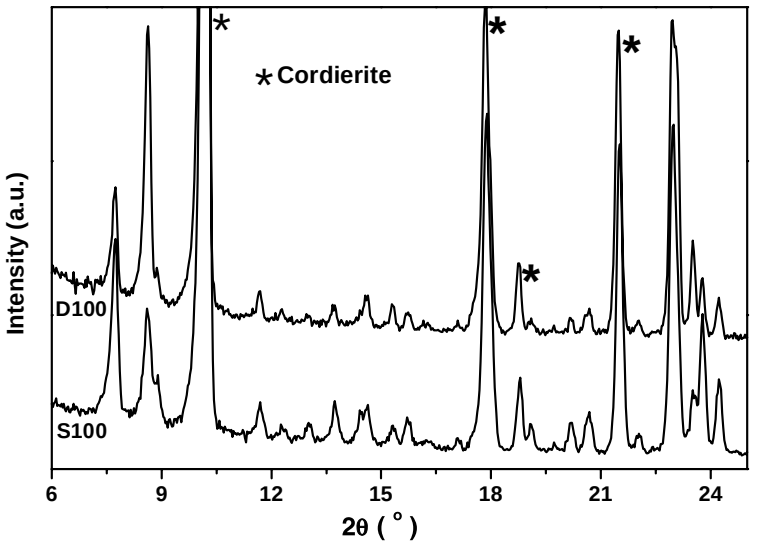

Fig. 2. X-ray diffraction patterns of ZSM-5 coated substrates: D100 (direct hydrothermal synthesis, Si/Al: 100) and S100 (secondary growth, Si/Al: 100). XRD cordierite signals are identified (✱).

characteristic hexagonal prism form were nucleated and grown on the unseeded substrate during in situ hydrothermal synthesis. A successive accumulation of ZSM-5 crystals lead to a scarcely intergrown polycrystalline film, with the [0 1 0] face of the coffin-shape crystals (*ac*-plane) preferentially parallel to the substrate surface in agreement with reports on ceramic membrane synthesis [22,23]. However, some twinned crystals are also observed (Fig. 3b) where the second crystal grows with the mentioned face (*ac*-plane) perpendicular to the surface of the first crystal (mother crystal) [24].

The microstructures presented in Fig. 4 correspond to the S100 sample, prepared by secondary (seeded) growth. In this case, a largely intergrown polycrystalline film with a columnar structure was obtained. The base layer of this film is a zeolite layer approximately 1.5 μm thick, with the [1 0 1] face (*c*-axis) preferentially oriented perpendicular to the surface of the substrate (Fig. 4c). Numerous lumps of zeolitic material can be observed on top of this layer, which probably originated from zeolite particles that nucleated in the bulk of the solution and after reaching a certain size precipitated onto the growing zeolite film. Also, some hemispherical dome-type defects were formed. According to Xomeritakis et al. [23] these defects are caused by gaps in the seed layer covering the support. In this case, however, the cordierite monolith surface is much rougher than the supports used by Xomeritakis et al. [23]. Thus, it seems likely that many of the irregularities observed also originate by local warps of the surface, that would induce initial crystal growth in multiple directions.

The preferential orientation of ZSM-5 crystals in the films obtained by seeded growth was also confirmed by XRD analysis. Thus, it can be seen that in the XRD patterns of D100 and S100 films (Fig. 2), the relative signal intensities in the 2θ range: 6°–9° and 22°–25° are notably different. It is possible to describe the tendencies on the crystal axis orientation of the film by analyzing the relative intensities of characteristic ZSM-5 peaks that are enhanced (or decreased) compared to ZSM-5 powder, in which a random distribution of crystal orientations is expected. Crystallographic Preferred Orientation (CPO) values were calculated according to the following equation [24,25]:

$$\mathrm{CPO}\left(\frac{[X]}{[Y]}\right) = \frac{I_S^{[X]}/I_S^{[Y]} - I_P^{[X]}/I_P^{[Y]}}{I_S^{[X]}/I_S^{[Y]}}$$

where "CPO([*X*]/[*Y*])" is the crystallographic preferred orientation based on the [*X*] and [*Y*] peaks. "*I*"

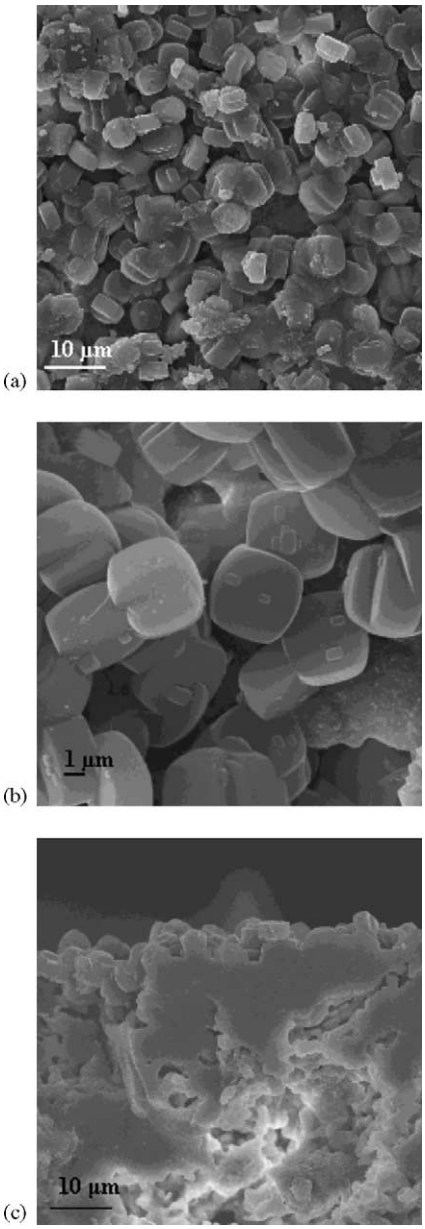

Fig. 3. Morphology of D100 sample (direct hydrothermal synthesis, Si/Al: 100). (a–b) Top view of surface and (c) cross–section.

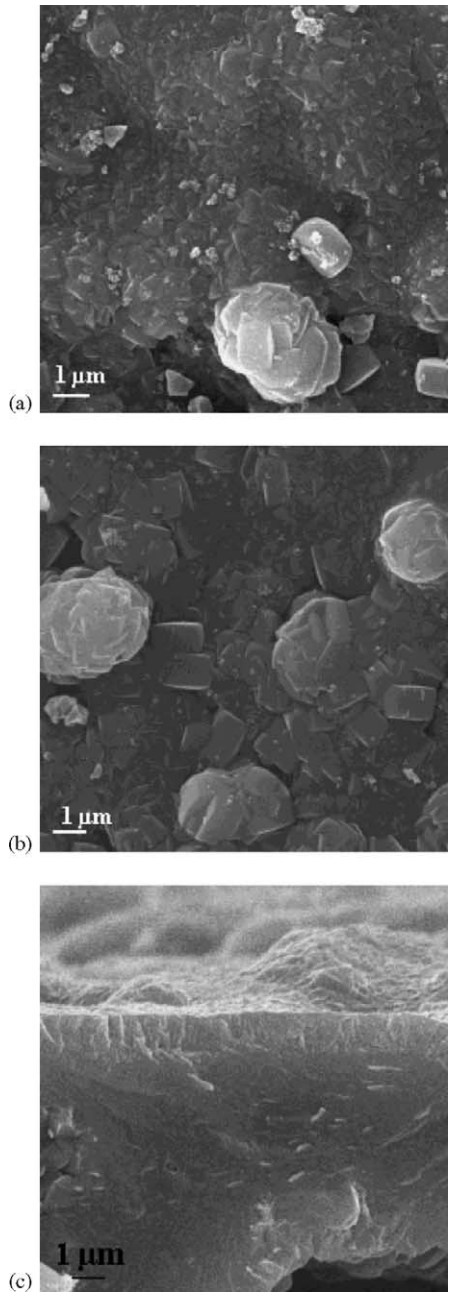

Fig. 4. Morphology of S100 (secondary growth, Si/Al: 100). (a–b) Top view of surface and (c) cross-section.

refers to the integral intensity of a peak, whereas "P and S" indicate the reference powder and the film coated substrate, respectively.

A CPO([051]/[501]) close to 1 would indicate that the majority of the crystals are oriented with *a*-axis ([0 1 0] face) parallel to the support [24,25]. In analogy with this, a CPO value for [002]/([200] + [020]) around 1 would indicate that most of the crystals are oriented with their *c*-axis perpendicular to the substrate surface. On the other hand, CPO(([200] + [020])/

Table 3
Crystallographic preferred orientation

Film coated substrate	CPO([051]/[501]) (b ⊥)	CPO([+]/[133])[a] (a or b ⊥)	CPO([002]/[+])[a] (c ⊥)	CPO([501]/[133]) (a ⊥)
D100	0.86	0.86	−0.20	0.49
S100	0.44	0.47	0.62	0.19
S100,14	0.49	0.29	0.69	−0.27

[a] [+] corresponds to ([200] + [020]).

[133]) describes the fraction of crystals oriented with either *a*- or *b*-axis perpendicular to the surface and CPO([501]/[133]) close to 1 is associated with *a*-axis perpendicular to the substrate. These four CPO values were calculated from the XRD data obtained on our samples and the results are reported in Table 3.

For sample D100, the CPO([051]/[501]) and CPO(([200] + [020])/[133]) values are close to 0.9 suggesting that the most of the coffin-shape crystals are oriented with *ac*-plane ([0 1 0] face) parallel to the substrate surface; this agrees with a negative value for CPO([002]/([200] + [020])) (perpendicular *c*-axis). Some contribution of crystals with *a*-axis perpendicular to the surface is expected because of its CPO([501]/[133]) value (Table 3). This effect is attributed to the presence of twinned crystals in which the *a*-axis of the secondary crystal is perpendicular to the *a*-axis of the mother crystal [22]. In this way, the CPO analysis for the XRD data obtained on D100 is in good agreement with the morphology observed by SEM (Fig. 3).

The crystals making up the coating for the S100 sample, prepared by secondary growth, appear to have a less marked orientation, according to the results in Table 3. Some coffin-shape grains with *ac*-plane parallel to the surface are present since the CPO([051]/[501]) and CPO(([200] + [020])/[133]) values are around 0.45. However, a CPO([002]/([200] + [020])) value equal to 0.62 indicates an important contribution of crystals with *c*-axis perpendicular to the surface, as expected for a film prepared by secondary growth. This is in agreement with the columnar grains observed by SEM at the base layer of the S100 film (Fig. 4c).

The Si/Al ratios for the S100 samples were estimated using EDX at the edge and at the middle of the zeolite films, with the results shown in Table 4. In both cases the Si/Al ratio is higher than in the synthesis gel (Si/Al = 100). Thus, in spite of some uncertainty regarding the values given (since the concentration of Al in the analyzed volume was close to the detection limit), it can be concluded that the incorporation of Al from the cordierite substrate into the zeolite film does not take place significantly under the synthesis conditions used. Finally, as shown in Table 2, the specific surface of the zeolite material in the samples prepared by secondary growth, S100, is about 15% larger than their directly synthesized counterparts (D100). This trend was also observed for the samples prepared with gels of Si/Al = 35 (see Table 2), and can probably be explained as a result of the higher crystallinity of the samples prepared by secondary (seeded) growth.

3.3. ZSM-5 coated substrates: Si/Al = 35

From the results presented in Fig. 5 it can be seen that the characteristic XRD signals for ZSM-5 (2θ range: 6°–9° and 22°–25°) are present, thus the formation of this phase takes place in samples D35, S35 and S35V. However, the XRD patterns in Figs. 2 and 5 clearly indicates a lower crystallinity for all the samples prepared with a gel with a Si/Al ratio of 35 in comparison to those obtained with Si/Al ratio = 100.

Fig. 6a shows different SEM micrographs for samples S35 and D35. The film morphologies of both samples are similar, consisting of a gel-like layer

Table 4
Si/Al ratio observed by EDX in the S100 and S35 samples

Film coated substrate	Si/Al precursor	Area	Si/Al film
S100	100	Border	122[a]
		Middle	227[a]
S35	35	Border	33
		Middle	71

[a] Aluminum amount was close to the detection limit.

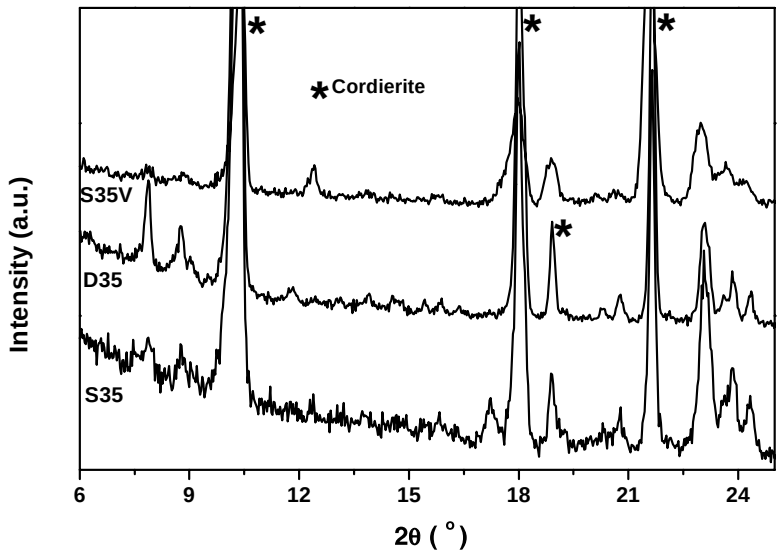

Fig. 5. X-ray diffraction patterns of ZSM-5 coated substrates: D35, S35 and S35V. XRD cordierite signals are identified (✱).

with small embedded microcrystals. Some crystals reached a larger size (several microns), especially in sample D35, although a nearly spherical crystal shape was maintained. The sample was treated with steam at 180 °C for 8 h (S35V), in an attempt to induce further zeolitization of amorphous material under a steam atmosphere. It can be seen that a remarkable change in the morphology of the gel-like layer takes place (Fig. 6b), together with a small reduction of the specific surface area (Table 2). However, this is not accompanied by a significant increase of crystallinity, as shown by the XRD patterns presented in Fig. 5.

In summary, the comparison of the SEM and XRD results for the films obtained with Si/Al ratios of 100 and 35, respectively, indicate that the gel layer formation on the substrate surface is favored by an increase of the Al content in the precursor solutions (i.e. as the Si/Al ratio decreased from 100 to 35). However, this higher Al content also decreased the zeolitization rate in the gel layer, in agreement with the results reported by Lai et al. [18]. Also, Nakamoto and Takahashi [26] and Giannetto et al. [27] reported that the presence of Al in the precursor solution decreases the zeolitization rate and Persson et al. [19] found that at low Si/Al ratio (<100) both, the nucleation and growth rates decreased notably.

At this point, it is important to remark that hydrothermal synthesis carried out in the absence of substrate but under otherwise similar conditions led to a well-crystallized ZSM-5 when a Si/Al ratio of 35 was used in the synthesis gel. Moreover, the powders obtained from the autoclave after film syntheses corresponded to a well-crystallized ZSM-5 phase (Fig. 1b). These results suggest that under the synthesis conditions used nucleation takes place predominantly in the bulk of the solution, rather than on the gel layer.

3.4. ZSM-5 coated substrate: Si/Al = 14

Both the films and powders obtained using a synthesis gel with this Si/Al ratio had essentially the same characteristics as described for those obtained with gels of Si/Al = 35. In summary, the zeolite films obtained can be described as a gel layer on the substrate surface with small crystals embedded on it, while the powder collected at the bottom of the autoclave had the characteristics of well-crystallized ZSM-5. As already mentioned for syntheses with Si/Al = 35, the nucleation rate in the bulk of the synthesis gel was faster than that in the gel layer, leading to crystal growth in the bulk solution rather than on the support.

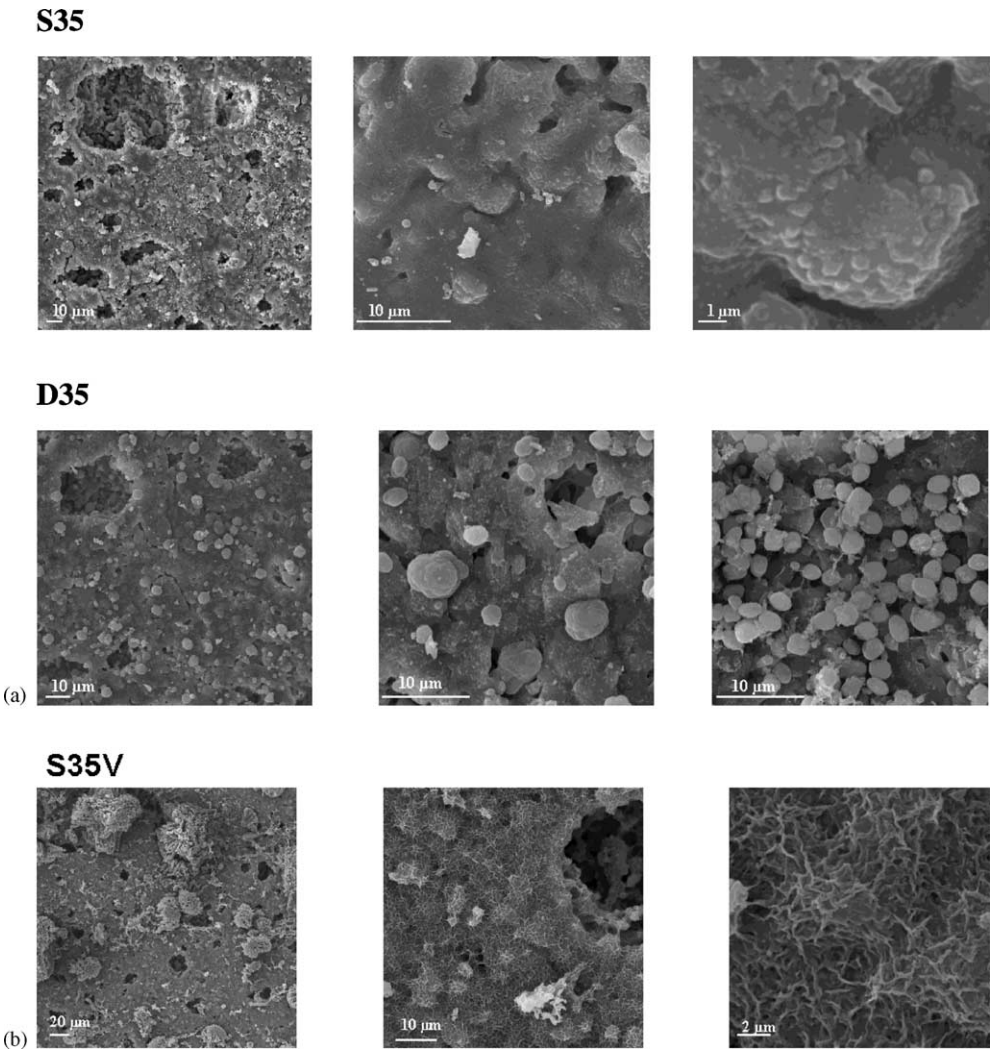

Fig. 6. (a) Surface morphology of samples D35 and S35; (b) surface morphology of sample S35V.

One possible solution to overcome this problem could be the growth of Al-rich films on top of Si-rich substrates, to help nucleation by providing an environment with a lower Al content. To this end, a Si-rich film was first prepared in a seeded synthesis, using a gel with a Si/Al ratio of 100. Then, a second (unseeded) synthesis was carried out using a gel with Si/Al = 14. Fig. 7 shows the morphology of this composite film, termed S100,14. It can be observed that the surface of the film (top view) after the second synthesis consists of tightly packed ZSM-5 crystals (7a), with a good degree of intergrowth (7b). Fig. 7c presents a view of the cross-section, where an apparently continuous zeolite layer has been formed in spite of the strong surface roughness of the support. In the close-up view of the cross-section (7d) two distinct layers can be observed: a lower layer corresponding to the Si/Al = 100 film with the characteristic columnar structure of films formed in seeded synthesis, and an upper layer, corresponding to the second synthesis with Si/Al = 14 in the gel.

Fig. 8 presents the variation of the Si/Al ratio of sample S100,14 across the film thickness, starting from the support (cordierite). Two different profiles

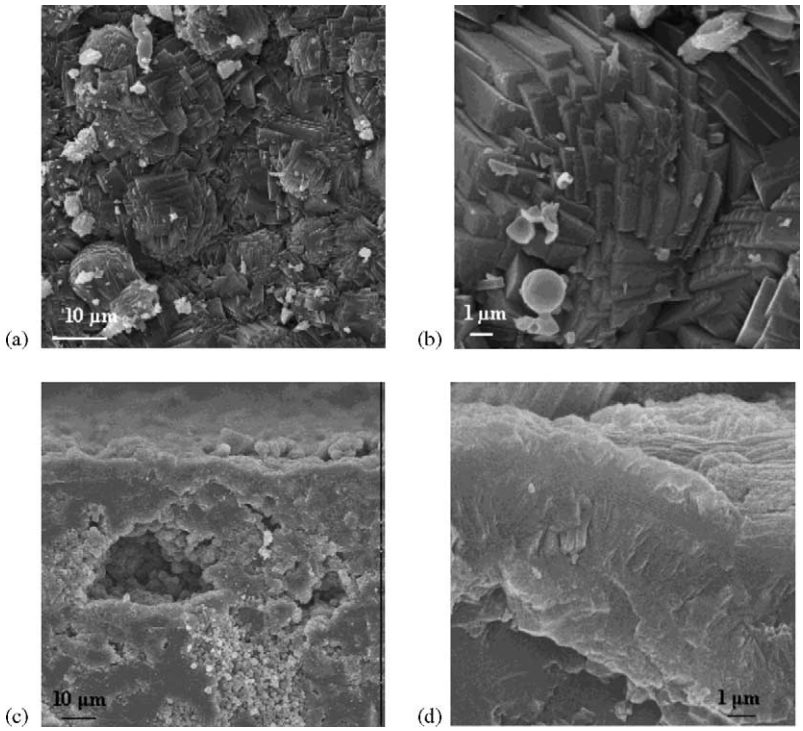

Fig. 7. Morphology of S100,14 film: (a–b) top view of surface; (c–d) cross-section.

are shown, corresponding to measurements at two locations of the support where very different film thickness were obtained (15 and 25 μm), due to the roughness of the support. In both cases, the Si/Al ratio reaches its maximum value towards the middle of the films, but this maximum is considerably lower than the Si/Al value of 100 existing in the gel during the synthesis of the first layer. It has already been shown (Table 4) that for the films prepared on cordierite using a synthesis gel with Si/Al = 100 the Si/Al values obtained by EDX were higher than 100. This means that the decrease in Al content of the first zeolite layer probably takes place during the synthesis of the second layer, using a Si/Al = 14 gel, by partial dissolution of the already formed layer.

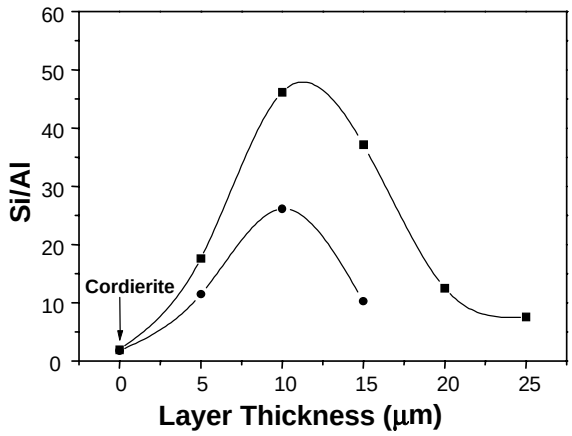

Fig. 8. Si/Al atomic ratio as a function of the distance from the support surface for sample S100,14. (*Note*: the cordierite support has a nominal Si/Al ratio of 2.5).

The SEM cross-sections (back-scattered electrons) shown in Fig. 9 for the S100,14 sample indicate a relatively homogeneous and continuous film, even though considerable variations of thickness are possible, as already indicated, due to the roughness of the support (see Fig. 9a). Most of the film, however, lies in the 15–20 μm thickness range (Fig. 9). In addition, a good adherence between ZSM-5 film and cordierite substrate was achieved in this preparation, and the films obtained were mechanically stable even after 20 min in an ultrasound bath. The films were also

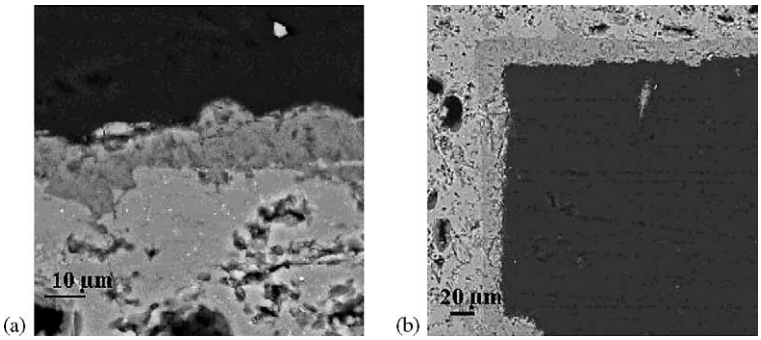

Fig. 9. Cross-section views of S100,14 film on monolith supports (back-scattered SEM).

stable against thermal cycling. To test this, the zeolite coated monoliths were first subjected to calcination in air at 400 °C for 8 h, then cooled down to room temperature and heated again to 550 °C, with 45 min dwell times at 300, 350, 400, 450, 500 and 550 °C. The sample was then cooled again to room temperature, heated to 550 °C, cooled to room temperature and weighted. There was no weight change, meaning that no zeolite material was lost in measurable amounts. Finally, the S100,14 film presented high crystallinity according to the XRD results of Fig. 10. In this case random orientation seems to dominate, although the value of CPO([002]/([200] + [020])) = 0.62 (Table 3) indicates some contribution of crystals with their *c*-axis perpendicular to the surface, probably a contribution from the first layer of crystals with a columnar *c*-oriented structure.

It is worth mentioning the recent work of Li et al. [28], who also prepared MFI layers of varying composition (termed "zoned" films) by a two-step crystallization procedure. In this case they used seeded synthesis on polished silicon and quartz substrates. These authors were able to grow zeolite films with high Al content (Si/Al = 10) either by seeded synthesis directly

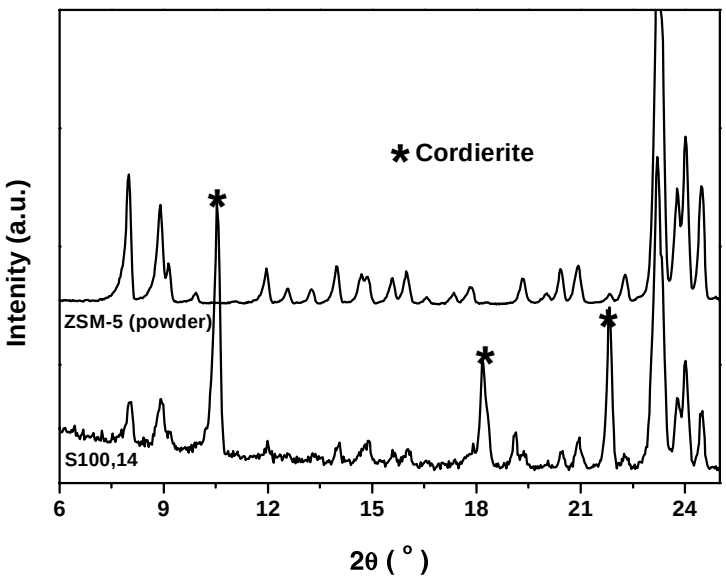

Fig. 10. X-ray diffraction patterns of ZSM-5 coated substrate, S100,14 in comparison to ZSM-5 powder. XRD cordierite signals are identified (✱).

on these substrates, or on previously formed silicalite layers, i.e. in both cases on Si-rich substrates. In most cases the second zeolite layer re-nucleated at the surface of the first layer, even when no seed crystals were planted at the interface between the first and second layers. A smooth transition was found, however, when the synthesis conditions of the second layer favored the growth of existing crystals, rather than nucleation at the surface. In our case, the first layer grown under Si/Al = 100 would be expected to provide a Si-rich environment for the nucleation and growth of the second layer under Si/Al = 14. The cross-section micrograph of sample S100,14 shows that this was the case: the interface between the two layers can be clearly observed (Fig. 7d), indicating that new nucleation processes occurred at the edge of the first layer, rather than a continuation of the growth of existing crystals. Given the large difference in the composition of both gels used in our work it seems likely that the top of the first layer (Si/Al = 100) would partly dissolve in contact with the Si/Al = 14 gel, helping in the nucleation of the second layer. This process would be favored at the higher temperature employed for the second synthesis (180 °C).

4. Conclusions

The composition of the precursor gels and the synthesis conditions used to prepare ZSM-5 coatings on monolith supports have a direct influence on the characteristics (morphology, crystal orientation, crystallinity) of the zeolite films formed. In particular, the formation of crystalline zeolite coatings of a high Al content (a desirable feature for many catalytic applications) is hindered by the presence of an Al-rich support, such as cordierite, even though Al from the cordierite does not seem to be significantly incorporated into the zeolite coating under the conditions used in this work.

The results of this study show that one way to circumvent this problem is the combination of two synthesis cycles using different Si/Al ratios. In a first synthesis, a high Si/Al ratio is used, to provide a suitable environment for the second synthesis using a gel with high Al content. The first layer is partly dissolved in the second synthesis gel, helping the nucleation and growth of the second layer. This has lead to high zeolite loadings (29 wt.%), with a low overall Si/Al ratio (Si/Al < 25 on average for the zeolite coating).

Acknowledgements

Financial support from MCYT, Spain, is gratefully acknowledged.

References

[1] H.P. Calis, A.W. Gerritsen, C.M. van den Bleek, C.H. Legein, J.C. Jansen, H. van Bekkum, Can. J. Chem. Eng. 73 (1995) 120.
[2] R.M. Heck, S. Gulati, R.J. Farrauto, Chem. Eng. J. 82 (2001) 149.
[3] F. Kapteijn, T.A. Nijhuis, J.J. Heiszwolf, J.A. Moulijn, Catal. Today 66 (2001) 133.
[4] J. Caro, M. Noack, P. Kölsch, R. Schäfer, Micropor. Mesopor. Mater. 38 (2000) 3.
[5] J. Coronas, J. Santamaría, Sep. Purif. Meth. 28 (1999) 127.
[6] E. Ito, R.J. Hultermans, H.P. Calis, J. C Jansen, H. van Bekkum, C.M. van den Bleek, Catal. Today 27 (1996) 123.
[7] C.D. Madhusoodana, R.N. Das, Y. Kameshima, A. Yasumori, K. Okada, Micropor. Mesopor. Mater. 56 (2001) 249.
[8] E.I. Basaldella, A. Kikot, C.E. Quincoces, M.G. Gonzalez, Mater. Lett. 51 (2001) 289.
[9] G.B.F. Seijger, O.L. Oudshoorn, A. Boekhorst, H. van Bekkum, C.M. van den Bleek, H.P.A. Calis, Chem. Eng. Sci. 56 (2001) 849.
[10] J.C. Jansen, J.H. Koegler, H. van Bekkum, H.P.A. Calis, C.M. van den Bleek, F. Kapteijn, J.A. Moulijn, E.R. Geus, N. van der Puil, Micropor. Mesopor. Mater. 21 (1998) 213.
[11] G.B.F. Seijger, O.L. Oudshoorn, W.E.J. van Kooten, J.C. Jansen, H. van Bekkum, C.M. van den Bleek, H.P.A. Calis, Micropor. Mesopor. Mater. 39 (2000) 195.
[12] J. Sterte, J. Hedlund, D. Creaser, O. Öhrman, W. Zheng, M. Lassinantti, Q. Li, F. Jareman, Catal. Today 69 (2001) 323.
[13] H. Kalipcilar, S.K. Gade, R.D. Noble, J.L. Falconer, J. Membr. Sci. 210 (2002) 113.
[14] M.C. Campas, B. Iacono, D. Pietrogiacomi, V. Indovina, Catal. Lett. 66 (2000) 81.
[15] J. Dêdecêk, D. Kauchý, B. Wichterlová, Micropor. Mesopor. Mater. 35 (2000) 483.
[16] J. Ramallo, F. Requejo, L. Gutiérrez, E. Miró, Appl. Catal. B: Environ. 29 (2001) 137.
[17] R. López-Fonseca, B. de Rivas, J.I. Gutiérrez-Ortiz, A. Aranzabal, J.R. González-Velasco, Appl. Catal. B 41 (2003) 31.
[18] R. Lai, Y. Yan, G.R. Gavalas, Micropor. Mesopor. Mater. 37 (2000) 9.
[19] A.E. Persson, B.J. Shoeman, J. Sterte, J.-E. Otterstedt, Zeolites 15 (1995) 611.
[20] J. Coronas, J.L. Falconer, R.D. Noble, AIChE J. 43 (1997) 1797.

[21] K. Aoki, V.A. Tuan, J.L. Falconer, R.D. Noble, Micropor. Mesopor. Mater. 39 (3) (2000) 485.
[22] J.H. Koegler, A. Arafat, H. van Bekkum, J.C. Jansen, Stud. Surf. Sci. Catal. 105 (1997) 2167.
[23] G. Xomeritakis, A. Gouzinis, S. Nair, T. Okubo, M. He, R.M. Overney, M. Tsapatsis, Chem. Eng. Sci. 54 (1999) 3521.
[24] J. Hedlund, S. Mintova, J. Sterte, Micropor. Mesopor. Mater. 28 (1999) 185.
[25] S. Mintova, J. Hedlund, V. Valtchev, B.J. Schoeman, J. Sterte, J. Mater. Chem. 8 (1998) 2217.
[26] H. Nakamoto, H. Takahashi, Chem. Lett. (1981) 1739.
[27] G. Giannetto, F.D. Santos, R. Monque, R. Galiasso, Z. Gabelica, Zeolites 11 (1995) 719.
[28] Q. Li, J. Hedlund, J. Sterte, D. Creaser, A.-J. Bons, Micropor. Mesopor. Mater. 56 (2002) 291.